Available online at www.sciencedirect.com

SCIENCE DIRECT®

Polymer 47 (2006) 1091–1100

polymer

www.elsevier.com/locate/polymer

Polyurethane elastomers with amide chain extenders of uniform length

Martijn van der Schuur [1], Bart Noordover [2], Reinoud J. Gaymans *

University of Twente, P.O. Box 217, 7500 AE Enschede, The Netherlands

Received 27 July 2005; received in revised form 15 November 2005; accepted 27 November 2005

Abstract

Toluene diisocyanate based polyurethanes with amide extenders were synthesized poly(propylene oxide) with a number average molecular weight of 2000 and endcapped with toluene diisocyanate was used as the polyether segment. The chain extenders were based on poly(hexamethylene terephthalamide): hexamethylene diamine, bisamine-diamide and bisamine-tetra-amide. The linear poly(ether bisurethane-bisurea-amide)s (PUA) were colorless transparent thermoplastic elastomers with a high molecular weight. The polymers were analyzed by IR and DSC, the morphology studied by TEM, the mechanical properties studied by DMTA and the tensile, the elastic properties by compression and tensile set and thermal stability by melt rheology.

The phase separation with these amide extenders was by crystallization. Increasing the length of the amide chain extender increased the modulus and the melting temperature of the PUA without changing the good low temperature properties. Also the elastic properties improved with amide segment length. The fracture stress increases with amide extender length. At 200 °C, the melt stability of the PUA with the bisamine-diamide chain extender was good.

Keywords: Polyurethane; Extender; Thermoplastic

1. Introduction

Linear polyurethane elastomers consist of alternating mobile polyether segments and rigid urethane or urea segments and are classified as thermoplastic polyurethanes (TPU's) [1–4]. Most rigid segments phase separate into hard domains dispersed in a soft matrix. These hard domains act as thermo-reversible physical crosslinks providing the characteristic thermoplastic and elastomeric behavior of the TPU-material [1].

The rigid segments can be present as crystallites, as liquid–liquid demixing particles and/or dissolved in the polyether phase. The rigid segments in TPU's are commonly synthesized from a 4,4′-methylenebis(phenyl isocyanate) (MDI) and a chain extender, which can be a diol or a diamine [2,3]. In most commercial TPU's (MDI based) diols, like butanediol, are used as chain extenders as with diamine extenders the resulting melting temperatures are often too high for melt synthesis and melt processing. In general the crystallinities of the hard segments are rather low and as a result the TPU's have rather low moduli [1]. TPU's bases on toluene diisocyanate (TDI) generally have compared to MDI based TPU's a lower modulus and lower melting temperatures this due to their lower crystalline order. The polyether and polyurethane segments are highly incompatible and liquid–liquid demixing is induced by increasing the rigid segment length [5,6]. The liquid–liquid demixed particles are however, not so effective in increasing the modulus [6]. Also the very short rigid segments remain dissolved in the polyether phase and increase the T_g of the polyether phase with as a result rather poor low temperature properties. Thus, neither dissolved rigid segments nor liquid–liquid demixed particles are wanted. Short segments that do not demix and do not remain dissolved are easily crystallisable segments with uniform length [7,8]. Polyurethanes with uniform length segments can be made in solution at low temperatures [9–12]. These materials have a lower polyether T_g and a higher modulus at room temperature than those having polydisperse (random) length crystallisable segments. The copolymers also have high fracture strains and high moduli at temperatures above the T_g, which on turn is little dependent on temperature. However, on melt processing above 180 °C, *trans*-urethane reactions occur and the uniform length distribution of the urethane segments are redistributed to a random length distribution [11,13].

---

* Corresponding author.
E-mail address: r.j.gaymans@utwente.nl (R.J. Gaymans).

[1] Present address: Océ-Technologies B.V., Venlo, The Netherlands.

[2] Present address: Technical University Eindhoven, Eindhoven, The Netherlands.

0032-3861/$ - see front matter © 2005 Elsevier Ltd. All rights reserved.
doi:10.1016/j.polymer.2005.11.074

Amide groups are more thermally stable than urethane groups and also amide-interchange reactions during high temperature melt polymerization hardly occur [14]. Exchanging some of the urethane groups in TPU's with amide groups decrease the urethane content and thereby might increase the thermal stability. By using amide extenders of random length the properties of polyurethanes are however, not improved: the polyether T_g was higher and the moduli lower [15].

Segmented blockcopolymers with uniform amide segments (polyether-amides) (PEEA) have high moduli combined with low T_gs of the polyether phase [7,8,16,17]. With uniform amide segments (diamide or tetra-amide) the crystallization is fast even at short segments length and the crystallization is almost complete as it takes place over the full length of the uniform amide segment. In addition, block copolymers containing only crystallized segments were found to be more elastic. Of the uniform amide segments studied, the longer tetra-amide segments were found to give block copolymers with a higher elasticity than those containing diamide segments.

The question is if uniform amide extenders are used in polyurethanes, do they also give block copolymers with a low T_g, high moduli, good elastic properties and improved melt stability.

Studied are segmented polyurethanes (PUA) based on poly(propylene oxide) end capped with 2,4-toluene diisocyanate ($TDI_{2,4}$) and diamine-amide extenders based on poly(hexamethylene terephthalamide) (nylon-6,T) (Fig. 1). These PUA block copolymers resemble previously studied polyether-amides with uniform amide segments based on nylon-6,T [17].

The diamine-amide chain extender length is varied ($x=0$–2): hexamethylene diamine (HMDA), 6T6 and 6T6T6. The properties of the PUA copolymers will be compared to a commercial polyether-urethane (TPU).

2. Experimental

2.1. Materials

Dimethyl terephthalate (DMT), hexamethylene diamine (HMDA), anhydrous *N*,*N*-dimethyl acetamide (DMAc), anhydrous *N*,*N*-methyl-2-pyrrolidinone (NMP), dimethyl formamide (DMF), toluene, *m*-xylene, osmium tetroxide (OsO_4), formaldehyde, chloroform, 1,1,1,3,3,3-hexafluoro-isopropanol (HFIP) and 2,4-toluene diisocyanate end capped poly(propylene oxide) $M_n=2300$ g/mol including the $TDI_{2,4}$ groups and 2000 g/mol for the PPO segment, (PPO_{2000}-$(TDI_{2,4})_2$) were purchased from Aldrich. Irganox 1330 was obtained from CIBA and *n*-butyl acetate from Merck. The $TDI_{2,4}$-terminated prepolymers were dried in vacuum at 70 °C overnight before use. All other chemicals were used as received. Diphenyl terephthalate (DPT) was synthesized as described before [14]. A commercial TPU (Desmopan KU-8672) was studied in detail before [18] and was a gift from Bayer AG (Germany).

2.2. Synthesis of 6T6-diamine-diamide chain extender

Hexamethylene diamine (278.1 g, 2.39 mol) and DMT (46.5 g, 0.24 mol) were introduced to a 1-l round bottomed flask equipped with reflux condenser, calcium chloride tube, magnetic stirrer, nitrogen inlet and thermocouple. The reaction was carried out without solvent at 80 °C. Within 1 h a white precipitate was formed. After 8 h, the white precipitate was filtered (glass filter, pore size 3) and subsequently washed three times with hot toluene (80 °C). The 6T6 diamine-diamide, was recrystallized from *n*-butyl acetate (20 g/1.5 l). Afterwards, it was washed three times with diethyl ether and thereafter dried in vacuum at 40 °C. Yield: 14.1 g (16%). Uniformity: >98% (by ^{1}H NMR). Longer $6(T6)_x$ segments were not detected by MALDI-TOF [14].

2.3. Synthesis of 6T6T6-diamine tetra-amide chain extender

The synthesis of 6T6T6-diamine tetra-amide was carried out in two steps. DPT (96.3 g, 0.30 mol) was dissolved in a mixture of 250 ml of *m*-xylene and 25 ml of DMF at 120 °C, which was placed into a 1-l round-bottomed flask equipped with reflux condenser, calcium chloride tube, magnetic stirrer, nitrogen inlet and thermocouple. Subsequently, HMDA (6.0 g, 0.05 mol) dissolved in 50 ml of *m*-xylene, was added to the DPT-solution. The reaction was carried out under continuous stirring at 120 °C for 12 h. The reaction mixture, containing the white precipitate T6T-diphenyl, was then filtered hot and thereafter washed with hot *m*-xylene (120 °C). Yield: 23.2 g (82%), purity 96% (by ^{1}H NMR).

T6T-diphenyl (22.6 g, 0.04 mol) and HMDA (93.0 g, 0.80 mol) were weighed into the reactor, i.e. the same setup as before and NMP (350 ml) was added as the solvent. At first the temperature of the reaction mixture was raised to 140 °C to dissolve the T6T-diphenyl, thereafter the reaction was stirred at 120 °C for 12 h. A white precipitate was formed, which was filtered and subsequently washed in chloroform at 50 °C (3*x*) and finally dried in vacuum at 40 °C. Yield: 23.5 g (97%). Uniformity: >96% (by ^{1}H NMR). The presence of very small amounts of 6T6T6T6 was detected by MALDI-TOF [14].

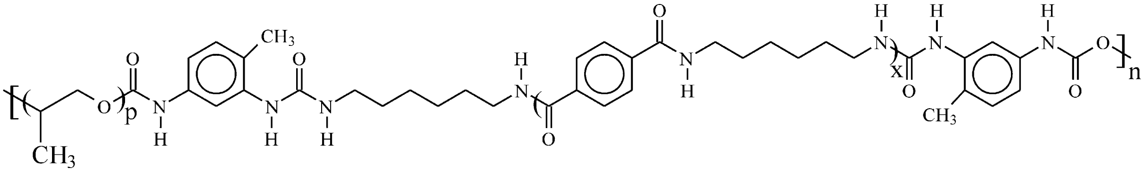

Fig. 1. Structure PUA-$6(T6)_x$ based on polypropylene oxide end caped with $TDI_{2,4}$ and extended with $6(T6)_x$.

2.4. Synthesis of polyether(bisurethane-bisurea-amide)s with uniform rigid segments

As an example the synthesis of PUA-6T6 with a chain extender length of $x=1$ is given. 6T6-Diamine diamide (3.66 g, 0.01 mol) and PPO-prepolymer (PPO_{2000}-$(TDI_{2,4})_2$) (23.2 g, 0.01 mol) were introduced to a 250 ml stainless steel reactor, fitted with glass lid, magnetic coupled stirrer and nitrogen inlet. The reactor was flushed with nitrogen. Irganox 1330 (antioxidant, 1 wt% of the prepolymer) and 80 ml anhydrous DMAc (solvent) were added. The reaction was carried out at 120 °C in an oil bath for 5 h under stirring. Thereafter, the solvent was stripped at 120 °C by applying a vacuum (pressure <0.4 mbar). After cooling the reactor the tough polymer was cut out of the reactor. The polymer was grinded and dried in a vacuum oven at 70 °C overnight.

PUA-6T6T6 ($x=2$) was synthesized using anhydrous NMP instead of DMAc. At the start of the reaction the temperature was raised to 150 °C for 30 min to dissolve the 6T6T6-diamine tetra-amide. Thereafter, the reaction was continued at 120 °C analogue to the synthesis of PUA with $x=1$.

2.5. Viscometry

The inherent viscosities of the block copolymers were measured using a capillary Ubbelohde (type OC) at 25°. Solutions of polymers in dimethylacetamide (DMAc) with a concentration of 0.1 g/dl were used.

2.6. FT-IR

Infrared absorbance spectra were recorded using a Biorad FTS-60. Samples of the polymers were first dissolved in HFIP. Afterwards, thin polymer films were cast on pressed KBr tablets. After evaporation of the solvent the infrared spectra were recorded.

2.7. Transmission electron microscopy (TEM) [19]

A small drop (40 μl) of a 0.3 wt% solution of polymer in HFIP was cast on a carbon coated copper grid (200 mesh). Subsequently, the grid with polymer film was heated at 20 °C/min to 20 °C above the flow temperature and kept for 5 min at this temperature using a DSC apparatus. After that, the material was allowed to cool at 3 °C/min to 40 °C below the melting temperature. Annealing at this temperature was conducted for 10 min after which the sample was allowed to cool to room temperature at 3 °C/min (this special heat treatment was necessary to erase any solvent effects generated during casting and to allow crystallization, if any in these ultra-thin films). The heat treated films were stained by immersing in 1 wt% osmium tetroxide/formaldehyde solution for 1 h at 40 °C. TEM measurements were performed with a Phillips CM30 at an accelerating voltage of 300 kV.

2.8. Melt processing

Test specimens, bars of $70\times 9\times 2$ mm^3, were prepared by injection molding using an Arburg H manual injection-molding machine. The barrel temperature was set to ±40 °C above the flow temperature as measured by DMTA. PUA-6T6T6 ($x=2$) copolymers had too high a melting temperature for injection molding and were compression molded to plaques of $120\times 120\times 2$ mm^3 on a Lauffer 40 press for 5 min at a pressure of 85 bar and a temperature of 200 °C.

2.9. Shore A hardness

A Zwick HHP 2001 shore A meter (ISO R 868/DIN 53505) was used to measure the hardness of the polymer samples in time directly after injection molding. The shore A hardness was acquired as the average of five measurements performed on different locations of the sample.

2.10. Dynamical mechanical thermal analysis (DMTA).

The storage (G') and loss modulus (G'') as function of temperature were measured on injection molded test bars ($70\times 9\times 2$ mm^3) using a Myrenne ATM3 torsion pendulum at a frequency of 1 Hz (at ~0.1% strain). The samples were first cooled to −100 °C and then subsequently heated at a rate of 1 °C/min. As glass transition temperature was taken the temperature at the maximum of the loss modulus. The flex temperature (T_{flex}) is defined as the temperature at the start of the rubber plateau region, the intercept of the tangents. The flow or softening temperature (T_{flow}) was defined as the temperature where the storage modulus reached 1.0 MPa.

2.11. Tensile

The tensile properties were determined on injection moulded bars cut to dumbbells (ISO 37 type 3). A Zwick Z020 universal tensile tester equipped with a 500 N load cell was used. The tensile tests were conducted at strain rate of 0.033 s^{-1}.

2.12. Compression set

Samples for compression set measurements were cut out from injection and compression molded bars. The compression set was measured according to the ASTM 395 B standard. After 24 h at room temperature the compression (25%) was released at room temperature. After half an hour, the thickness of the samples was measured. The compression set was defined as:

$$\mathrm{CS}=\frac{d_0-d_2}{d_0-d_1}\times 100\% \qquad (1)$$

d_0, thickness before compression (mm); d_1, compressed thickness (mm) (here $d_1=1.65$ mm); d_2, thickness 30 min after release of compression (mm).

Table 1
Properties of PUAs

Extender	x	RS content[a] (wt%)	RS content[b] (wt%)	η_{inh} (dl/g)	T_m (°C)	ΔH_m (J/g)	T_g (°C)	T_{flex} (°C)	T_{flow} (°C)	G' (25°C) (MPa)	CS (%)
-6-	0	19.3	9.8	0.58	90	1.2	−51	−25	103	4.4	15
-6T6-	1	26.7	18.4	0.58	166	10.8	−53	−34	169	13	10
-6T6T6-	2	32.9	25.5	0.35			−55	−29	264	16	6.2
TPU [18]	–	–	–	–			−45	−10	150	11	13[c]

[a] Rigid segment content including the TDI linkages.
[b] Rigid segment content excluding the TDI linkages.
[c] Measured at 55% compression [18].

CS-values were calculated as the average of three measurements.

2.13. Tensile set

To measure the tensile set of the block copolymer samples, cyclic stress–strain experiments were conducted on injection molded bars cut to dumbbells (ISO 37 type 3). A Zwick Z020 universal tensile machine equipped with a 500 N load cell was used to measure the stress as function of strain for each loading and unloading cycle at a strain rate of $3.33\times10^{-2}\ \mathrm{s}^{-1}$ (test speed of 50 mm/min). The strain of each loading–unloading cycle was increased (stair-case loading) and the tensile set was determined as function of the incremental strain. The incremental tensile set was calculated from the following relation:

$$\text{Tensile set} = \frac{\Delta\varepsilon_{\text{remaining}}}{\Delta\varepsilon_{\text{cycle}}} = \frac{\varepsilon_{r,\text{cycle}(i)} - \varepsilon_{r,\text{cycle}(i-1)}}{\Delta\varepsilon_{\text{cycle}}} \times 100\% \qquad (2)$$

With $\varepsilon_{r,\text{cycle}(i)}$ the remaining strain at the end of cycle i and with $\varepsilon_{r,\text{cycle}(i-1)}$ the remaining strain at the end of the preceding cycle $i-1$. Direct after the stress was zero a new cycle was started and the strain steps were 10%.

2.14. Melt stability

The melt viscosity of polymer samples in time at a constant temperature and piston speed (5 mm/min, shear rate $57.5\ \mathrm{s}^{-1}$) was determined using a Kayeness capillary flow rheometer. The length and diameter of the capillary were, respectively, 20.32 and 1.016 mm. The inner diameter of the barrel was 9.525 mm. The force (F) necessary to push the melt through the capillary was measured, and the melt viscosity was calculated from:

$$\eta = \frac{F r_c^4}{8\pi R_b^4 L_c S} \qquad (3)$$

F, force on piston $(\mathrm{N}) = (\mathrm{Pa\ m}^2)$; r_c, inner radius of the capillary (m); R_b, inner radius of the barrel (m); L_c, length of capillary (m); S, piston speed $(\mathrm{m\ s}^{-1})$.

3. Results and discussion

Polyether(bisurethane-bisurea-amide)s (PUA) were synthesized from poly(propylene oxide) (PPO_{2000}) end capped with $TDI_{2,4}$ ($M_n = 2300$ g/mol including the TDI groups) and uniform diamine-amide chain extenders (Fig. 1). The extenders: hexamethylene diamine ($x=0$), 6T6-diamine ($x=1$) and 6T6T6-diamine ($x=2$), are all of uniform length as determined by MALDI-TOF [14]. The polymerizations were at a low temperature (120 °C) this to limit possible trans reactions. As each hard segment contains only two urethane groups, which are in symmetrical positions, it is expected that *trans*-urethanization, if taking place, does not lead to loss of uniformity of these segments.

3.1. Synthesis of PUA copolymers

The PUA copolymers with $x=0$ and 1, were colorless to slightly yellow transparent materials and had inherent viscosities of 0.58, indicating a high molecular weight (Table 1).

Literature values of inherent viscosities of segmented polyurethanes ranged from 0.25 up to 0.70 dl/g (0.1 g/dl in DMAc at 25 °C) [20,21]. With $x=2$, the block copolymer obtained was a non-transparent brownish material of low inherent viscosity (low molecular weight). The low molecular weight is probably due to poor solubility of the 6T6T6 extender units in the solvent during the reaction. The samples for testing for $x=0$ and 1 were made by injection molding, but for $x=2$ the melting temperature of the material was too high for injection molding and compression molding at 200 °C was used instead for the preparation of test bars. For $x=1$ samples the DMA's of injection moulded and compression moulded samples were very similar.

Properties of a commercial melt-processable TPU are also included (Table 1) [18]. This TPU has a similar modulus and flow temperature as the PUA-6T6.

3.2. FT-IR spectroscopy on PUA copolymers

Infrared spectroscopy is a common tool to study the hydrogen bonding in segmented polyurethanes and is also used for the PUA copolymers. In $TDI_{2,4}$-based PUA copolymers, three groups are present that can form H-bonds: urethane, urea and amide groups. The absorbance bands of the TDI based urethane and urea groups and amide groups in the free state and in the hydrogen bonded state, as reported in literature [21–25], are given in Fig. 2. For urea groups it is known that H-bonding can occur in two different forms: bidendate (strongest) and monodendate [22–25] (Fig. 2).

In the infrared spectrum of the PUA-6 copolymer for ν(N–H) a single peak is observed at 3291 cm^{-1} (hydrogen bonded) and for ν(C=O) peaks were observed at 1724 cm^{-1} (hydrogen bonded urethane), at 1700 cm^{-1} (free urea) and at 1682 and 1663 cm^{-1} (monodendate urea) (Fig. 3). No peaks of this spectrum can be assigned to bidendate hydrogen bonding ($\sim$1640 cm^{-1}) of the urea group.

The spectrum of the PUA-6T6 shows a single ν(N–H) peak at 3370 cm^{-1} for the non-hydrogen bonded and 3290 cm^{-1} for the hydrogen-bonded groups (shoulder). For ν(C=O) at 1783 and 1753 cm^{-1} (free urethane), 1709 cm^{-1}, (free urea), 1682 cm^{-1} (monodendate urea), a small shoulder at 1641 cm^{-1} for either the bidendate hydrogen bonded urea and/or amide hydrogen bonded. In the spectrum of PUA-6T6 no peak at 1725 cm^{-1} for the hydrogen-bonded urethane carbonyl was detected.

By incorporating amide groups to extend the urethane-urea segment, the absorbance bands are shifted to higher frequencies and, therefore, the urethane groups with the 6T6 extender are less hydrogen bonded. However, the peak intensity (at 1680 cm^{-1}) of the urea group's monodendate hydrogen bonding is stronger.

The occurrence of monodendate hydrogen bonding of urea groups and a large fraction of non-hydrogen bonded urethane groups is quite common for segmented polyether(urethane-urea)s containing $TDI_{2,4}$ groups [23].

A schematic packing of PUA-6T6 is given (Fig. 4). If there is strong hydrogen bonding between the amide groups than the hydrogen bonding of the urea group must be of the monodendate type. This seems to be confirmed with the IR bands. The positioning of the methyl group of the $TDI_{2,4}$ can either be at the urethane or urea side.

The reactivity of the isocyanate group at the C_4-position is much higher than at the C_2-positioned [26]. It is, therefore, expected that the urethane group in the $TDI_{2,4}$-PPO-$TDI_{2,4}$ prepolymer is at the C_4-position and thus the urea group in the copolymer at the C_2-position as given in Fig. 4. The methyl group is at the same side at the urea group and may cause sterically hindrance of the hydrogen bonding of the urea group. To accommodate hydrogen bonding in the urea group the methyl group might have turned the phenyl ring out of plane with regard to the urea group. Consequently, the urethane groups at the C_4-position are turned out of plane. As a result,

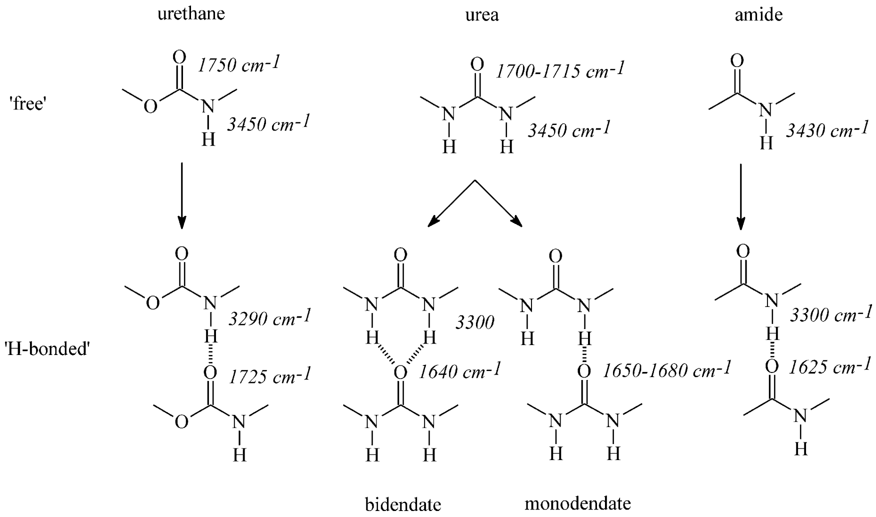

Fig. 2. Infrared absorption bands for hydrogen bonding (ν(N–H) and ν(C=O)) of TDI based urea, TDI based urethane and amide groups [21–25].

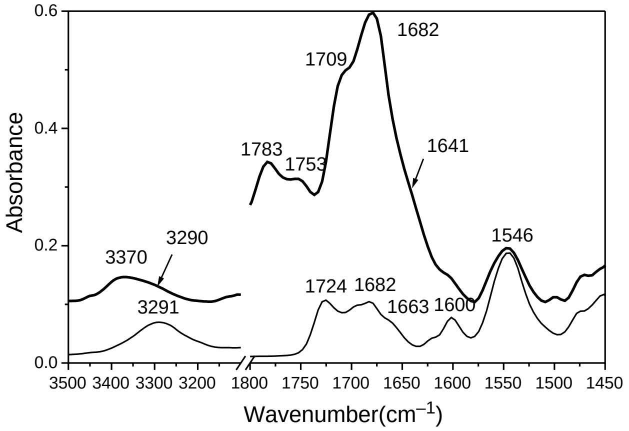

Fig. 3. IR-spectra of PUA block copolymers in wavenumber range: 3500–3100 cm^{-1}, 1800–1450 cm^{-1} with different extenders: bottom line, HMDA; top line, 6T6.

tight packing of the urethane group becomes difficult. The absence of hydrogen bonded urethane as observed with IR is thus logical. These results indicate that the $TDI_{2,4}$ units are not part of the crystalline phase. A clearer picture of the state of the TDI groups can be obtained with infrared dichroism [18].

In the PUA-6T6 both amide and monodendate urea hydrogen bonding is present. These PUA-6T6 copolymers probably contain four hydrogen bonds per rigid segment instead of the six hydrogen bonds that are possible.

3.3. Morphology

The morphology of the PUA-6T6 copolymer was studied by means of TEM on samples strained with OsO_4/formaldehyde (Fig. 5). With OsO_4/formaldehyde the amide groups were strained [8,15,17,19,27]. In segmented block copolymers with crystalline amide segments crystalline structures are observed both with TEM and AFM [8,17]. In segmented block copolymers that do not crystallize and phase separate by liquid–liquid demixing show with TEM spherical domains and no lamellar structures [6]. In the TEM micrograph of the PUA-6T6 copolymer ribbon structures of approximately 2–5 μm long and 50–200 nm wide can be observed. The thickness of the crystallites is expected to be in the order of 4 nm. The aspect ratio of the crystallites is then 500–1250. The width (in the non-hydrogen bonding direction) of 50–200 nm is larger than with amide segments [17]. This width is sensitive to the sample preparation procedures.

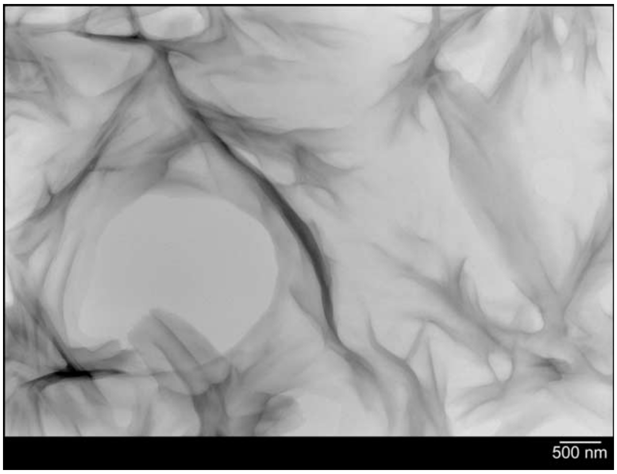

Fig. 5. TEM micrograph of PUA-6T6 copolymer stained with OsO_4/formaldehyde.

For PUA-6T6 no stained spherical domains as in liquid–liquid demixed systems were observed [6].

3.4. Hardening rate (crystallization)

The crystallization rates of PUA-6 and PUA-6T6 after injection molding are indirectly monitored by measuring the hardness (in shore A) as function of time (Fig. 6). Injection molding of the PUA-6T6T6 copolymer was not possible due to the high melting temperature, and its hardening rate was, therefore, not examined.

For PUA-6 the hardness increases gradually with time and levels off after 10,000 s (3 h), after which a slight increase in shore A is observed. At the end, a hardness of 65 shore A is obtained. The hardness of polymer PUA-6T6 is already at a high level after 10 s and increases little with time. The final hardness of the PUA-6T6 is approximately 85 shore A. By the incorporation of -6T6- as chain extender instead of hexamethylene diamine (-6-) the crystallization rate is strongly increased and the processing time (time to solidify) of the PUA is, therefore, reduced considerably. Also the hardness is appreciably higher.

3.5. Dynamical mechanical thermal analysis

Thermo-mechanical properties of the polymers were determined by means of DMTA. Despite the fact that segmented polyurethanes are thermally unstable at

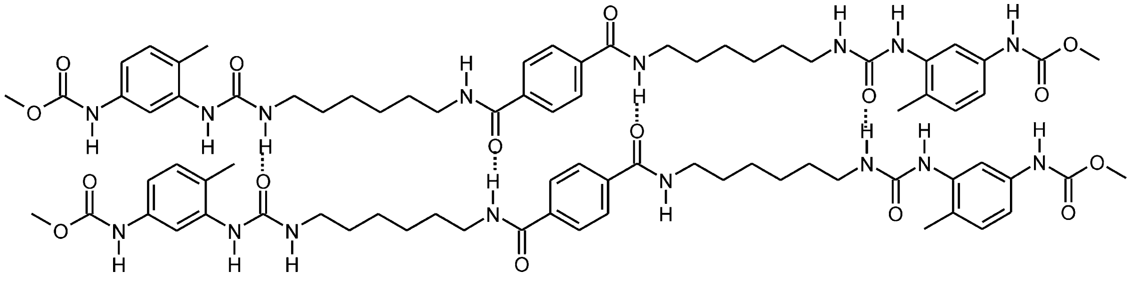

Fig. 4. Probable hydrogen-bonding in PUA-6T6 copolymers (the urethane groups are non-hydrogen bonded).

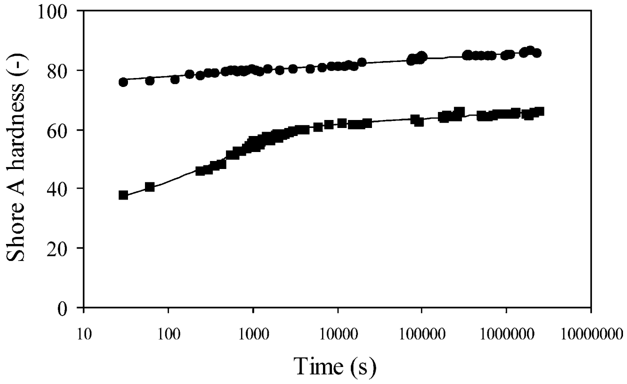

Fig. 6. Shore A as function of time after injection-molding for PUA with the extenders: (■), HMDA; (●), 6T6.

temperatures >180 °C it is assumed that the DMTA results are still of use. This is based on the fact that the DMTA experiments are conducted at small strains (0.1%). At low strains the effect of changes in molecular weight (due to degradation) on polymer properties is small. The storage and loss moduli of the PUA copolymers have been plotted as function of temperature (Fig. 7).

The DMTA graphs of the PUA copolymers exhibit sharp phase transitions and the modulus above the T_g has a small temperature dependence, as indicated by the low values of $\Delta G'$ (Table 1). The glass transition temperature (T_g) and flex temperature (T_{flex}) are low and decreases with increasing amide extender length. Thus with the longer extender units, the hard segments are less miscible with PPO. From the glass transition temperature of the copolymer the amount of dissolved hard segments in the PPO phase can be estimated. A poly(propylene oxide) with molecular weight of 2000 between crosslinks has a T_g of −60 °C [6,8,17]. The measured T_gs are −51 to −55 °C and the shift in T_g due to dissolved hard phase is in the order of 9−5 °C. From this shift, the amount of dissolved hard segments can be estimated with the Fox relationship [8,17,28]. If the T_g of the pure hard phase is assumed to be at about 200 °C then 9–5° shift suggest that about 9–5 wt% of hard phase is dissolved in the PPO. Consequently, when the phase separation in these copolymers occurs only by crystallization than 9–5 wt% hard segments is not crystallized.

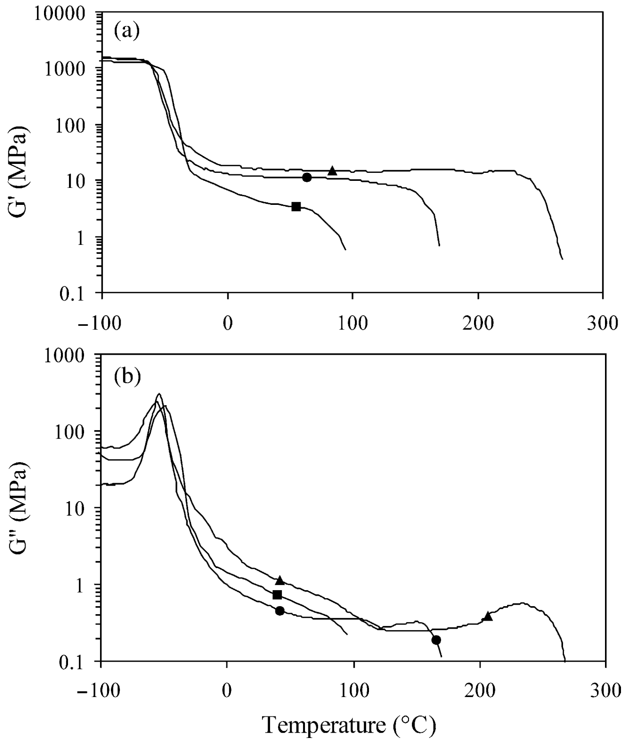

Fig. 7. The storage (a) and loss modulus (b) of PUA copolymers as function of temperature for the extenders: (■), HMDA; (●), 6T6; (▲), 6T6T6.

The DMTA of PUA-6T6 having uniform 6T6 units is compared to a commercial polyurethane (TPU) with a similar modulus at room temperature (Table 1, Fig. 8). The PUA-6T6 has a lower T_g, a lower T_{flex}, a modulus (above the T_g) that is less temperature dependent and a sharper melting transition than the commercial TPU. This suggests that the PUA-6T6 copolymer has a higher degree of phase separation and a more uniform crystalline morphology.

The flow temperatures (T_{flow}) measured by DMTA are close to the melting temperatures (T_m) as measured by DSC (Table 1). The melting temperatures of the PUA's were determined from the first DSC-heating scan of samples from melt processed bars. With increasing the chain extender length ($x=0\rightarrow 2$), the flow temperature of the corresponding polymer is increased from 103 to 264 °C. These flow temperatures are due to melting of the crystallized urea-amide phase, and the increase in flow temperature observed may be the result of an increasing in the thickness of the crystalline lamellae [7–9,17]. For the HMDA extended copolymer, the heat of melting is low and for the 6T6 extended copolymer higher but not exceptionally high. This also suggests that the hard segments in the copolymers have not fully crystallized.

The storage modulus of the PUA copolymers increases with extender length (Table 1, Fig. 7). The increase in storage modulus of segmented copolymers with crystallisable segments is due an increase in concentration of crystalline material and/or the aspect ratio of the crystallites [8,17]. This increase in modulus could be described by the fiber composite model of Halpin–Tsai [8,17,29]. The PUA copolymers have crystalline ribbons with a high aspect ratio (Fig. 5). The modulus of these

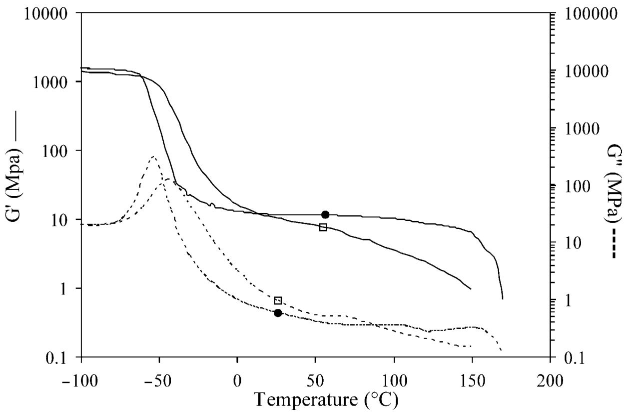

Fig. 8. DMTA graphs for (●) a PUA-6T6 copolymer and (□) a commercial TPU [18].

copolymers is plotted as function of the volume percent hard segments (black dots) (Fig. 9). Also given are the results of the Halpin–Tsai relationship [29]. From this figure it becomes clear that the PUA copolymers do not follow the Halpin–Tsai relationship probably due to the fact that the hard segments are not fully crystallized. The fact that the hard segments in the PUA copolymers were not fully crystalline was already concluded from IR experiments, as well as the T_g-shift and the heat of melting detected by DSC. Not all the hard segments may have crystallized and/or part of the hard segments did not crystallize. With IR we have seen that the urethane groups were not hydrogen bonded and this suggest that the $TDI_{2,4}$ groups had not crystallized. $TDI_{2,4}$ has an irregular structure and has a methyl group that sterical hinders a good packing. The hard segment content without the TDI groups are calculated (Table 1). The difference in hard segment content due to the $TDI_{2,4}$ groups corresponds well with the amount of dissolved hard segments in the polyether phase as calculated from the T_g shifts of the polyether. The modulus as function of crystalline volume fraction without the TDI groups (open dots) is also plotted (Fig. 9). These data nearly follows the Halpin–Tsai relationship. The modulus increase with hard segment content of the PUA with TDI groups reasonably can be well described by the composite model if assumed that the $TDI_{2,4}$ groups does not take part in the crystallization.

A more regular diisocyanate group than $TDI_{2,4}$ may result in a better packing of the urethane-urea segments, however, at the same time the melting temperature will increase.

3.6. Tensile properties

Tensile properties were only measured on PUA-6 and PUA-6T6 injection moulded samples. The copolymers were flexible materials with high fracture strains ($>600\%$) (Fig. 10).

The copolymer with the extenders HMDA and 6T6 had at 10% strains stresses of, respectively, 0.38 and 1.24 MPa. Clear yield points are not visible and the yield strain for HMDA and 6T6 are about at 70 and 50% strain. These yield strains are high and suggest that excessive plastic deformation starts at high strains, but the non-linearity of the stress–strain curve starts much earlier at 40 and 15%, respectively. Past the 'yield strain' the stresses increase gradually with strain, as is often seen in PPO copolymers. The fracture stresses are moderately high at 5.4 and 10.7 MPa, respectively. Increasing the extender length from HMDA to 6T6 has a strong effect on the stress at 10% strain and the fracture stress. The influence of the extender length on the fracture stress is remarkable strong.

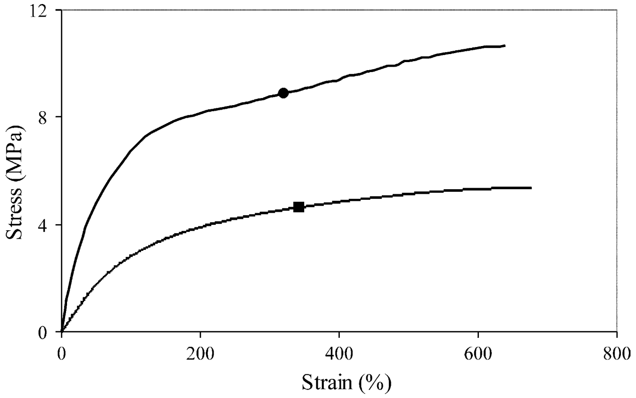

Fig. 10. Stress–strain behavior of PUA copolymers with different extenders: (■) HMDA; (●), 6T6.

3.7. Elasticity of PUA copolymers

3.7.1. Compression set

The elasticity of segmented block copolymers is commonly quantified by means of a compression set (CS) tests. Chemically cross linked polyurethanes have very low CS values [30] (high elasticity) and the compression set values of linear segmented block copolymers increases with increasing modulus [8,16–18]. However, with a particular soft segment length and increasing hard segment length, the modulus increases and the CS-values decreases [8]. The CS-values for the PUA copolymers are low (Table 1) and these materials are thus highly elastic. Increasing extender length even lowers the CS (15–6%) and this is due to the higher resistance to deformation of the thicker crystallites [17]. Thus with increasing extender length the modulus increases and the CS decreases (Fig. 11).

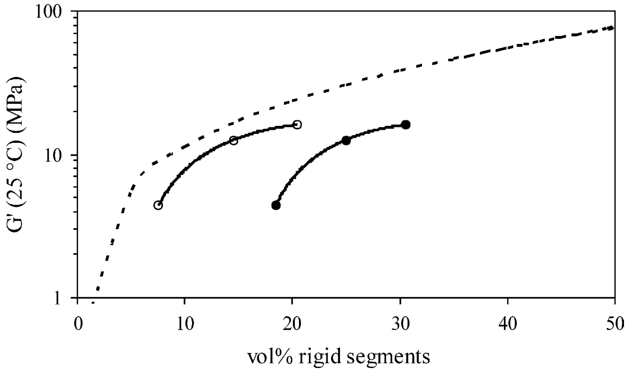

Fig. 9. Storage modulus ($G'_{25\ °C}$) as function of the concentration of uniform rigid segments of PUA copolymers: (●), including the TDI group; (○), excluding the TDI group. Dashed line: composite model [17,29].

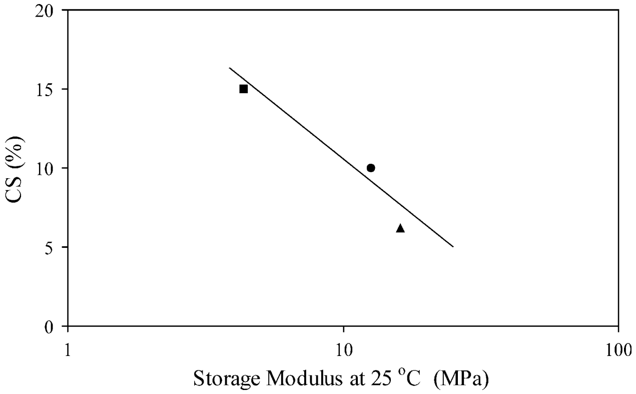

Fig. 11. Compression set (CS) as function of the storage modulus of PUA copolymers for the extenders: (■), HMDA; (●), 6T6; (▲), 6T6T6.

The observed CS as function of modulus of the PUA-6T6T6 copolymer approaches that of chemically cross linked polyurethane [30].

3.7.2. Tensile set

To gain insight in the process of deformation upon straining of the PUA copolymers, the incremental tensile sets (TS) of the polymers as function of strain were measured by cyclic tensile tests (stair-case loading) (Fig. 12). The PUA-6T6T6 copolymer ($x=2$) was too brittle and cyclic tensile measurements on this material were, therefore, not performed.

The tensile set of the PUA copolymers increases in the first 30% strain and thereafter leveled off. The plateau PUA-6 has a plateau region and this suggest that macroscopic yielding is taken place. For PUA-6T6 at strains above 30% a gradual increase in TS is observed. This behavior of gradual increasing TS values with increasing strain is a normal behavior for affine deforming systems.

The PUA-6T6 has in the region of 0–100% lower TS despite its higher modulus. These results are in line with the CS values. The use of the 6T6 chain extender instead of HMDA (6), improves the elasticity of the corresponding polymer combined with a higher modulus. Both the PUA-6 and PUA-6T6 copolymers have somewhat lower TS-values than similar PEEA's [17], which is in line with trends observed in the compression set.

3.8. Melt stability of PUA vs. commercial TPU

Segmented polyurethanes are known to be thermally instable in the melt: at temperatures above 180 °C the molecular weight of the copolymers decreases dramatically. At elevated temperatures (>150 °C), besides degradation reactions, also *trans*-urethanisation reactions may occur [2,13]. As a result of the interchange reactions, randomization of the segments takes place, while the molecular weight of the polymer remains unchanged. If the urethane segments were of uniform length then the trans reactions might be the cause of the loss of the uniform character of the segment. Amide units are more thermally stable and *trans*-amidation reactions are very slow. In the PUA copolymers *trans*-urethanization may take place. In the hard segments of PUA used the number of urethane groups is two and at symmetrical positions (Fig. 1). Due to the symmetrical positions a possible *trans*-urethanisation reaction is not expected to have an effect on the uniformity of the hard segments. Therefore, after melt processing the PUA copolymers still have the behavior of a block copolymer system with crystallisable units of uniform length.

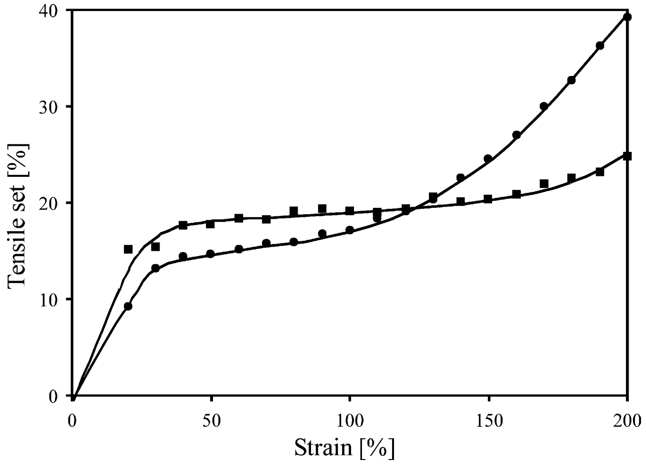

Fig. 12. Tensile set (TS) as function of strain for the extenders: (■), HMDA; (●), 6T6.

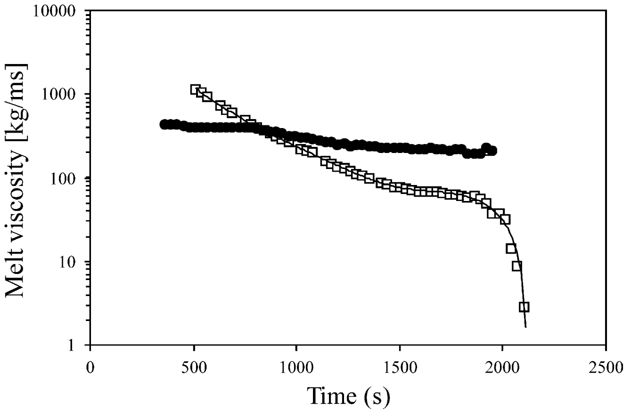

Fig. 13. The melt viscosity (η) as function of time at 200 °C: (●), PUA-6T6; (□), a commercial TPU.

The thermal degradation in the melt is studied by capillary rheometry (Fig. 13). The melt viscosity at 200 °C as function of time for the PUA-6T6 copolymer is determined.

The melt viscosity of PUA-6T6 copolymer decreases a little with time. The PUA-6T6 copolymer is thus at 200 °C fairly thermally stable. At these conditions the melt viscosity of a commercial TPU is also studied. The viscosity of the TPU decreases strongly with time. The higher thermal stability of the PUA-6T6 copolymer is probably due to the use of more thermally stable amide-based chain extenders and the (much) lower concentration of urethane groups.

4. Conclusions

Poly(ether bisurethane-bisurea-amide)s (PUA) were synthesized from PPO_{2000} end capped with $TDI_{2,4}$ groups and chain extended with uniform diamines containing amide groups (-PPO_{2000}-TDI-6(T6)$_x$-TDI-). The repetitive length x of the chain extenders was increased from 0 to 2, i.e. hexamethylene diamine, 6T6-diamine and 6T6T6-diamine. At chain extender lengths of $x=1$ and 2, amide groups are incorporated. The block copolymers with $x=0$ and 1 were colorless to slightly yellow transparent materials with high molecular weights.

As judged by IR, the hydrogen bonding was not taking place in the urethane groups and not in the urea bidendate state. The irregular structure of the $TDI_{2,4}$ limits the hydrogen bonding of the TDI-group.

With the 6T6 extender the phase separation was by crystallization and the crystalline ribbons had a high aspect ratio. Using the 6T6 extender the crystallization rate of the block copolymer was high and also higher than for block copolymer with the HMDA extender.

Increasing the chain extender length increased the storage modulus and flow temperature of the corresponding copolymers and all this combined with lower compression and tensile set values. The modulus in the plateau region, i.e. the rubber region, is little temperature dependent. The increase in modulus can be modeled by the increase in crystallinity if assumed that the $TDI_{2,4}$ groups are not take part in the crystallization. With increasing extender length the stress at 10% strain and the fracture stress increases. The lower CS and TS values with increasing extender length are thought to be due to the increased resistance to deformation of the thicker crystallites. The low T_g and T_{flex} temperatures suggest a good phase separation particularly for $x=1$ and 2. The melt stability of PUA-6T6 at 200 °C is good, which may be due to the low urethane group content.

The use of the diamine-diamide extender (-6T6-) in polyurethanes enhances the modulus and elastic properties, this combined with at a low T_g and even the thermal stability is good.

Acknowledgements

This research was financed by the Dutch Polymer Institute (DPI), The Netherlands. The authors would like to thank Professor Dr J. Feijen and Dr E. van der Heide from Shell Amsterdam and Dr H.J.M. Gruenbauer for DOW Terneuzen for their discussions.

References

[1] Holden G, Legge NR, Quirk R, Schroeder HR. Thermoplastic elastomers. 2nd ed. Munich: Carl Hanser Verlag; 1996.
[2] Bayer O. Mod Plast 1947;24:250.
[3] Frisch KC, Saunders JH. Polyurethanes: chemistry and technology. Part I. Chemistry. In: Mark H, Flory PJ et al, editors. High polymers, vol. 16. New York: Wiley; 1964.
[4] Frisch KC, Saunders JH. Polyurethanes: chemistry and technology. Part II. Technology. In: Mark H, Flory PJ et al, editors. High polymers, vol. 16. New York: Wiley; 1964.
[5] Leibler L. Macromolecules 1980;13:1602.
[6] van der Schuur M, van der Heide E, Feijen J, Gaymans RJ. Polymer 2005; 46:3616.
[7] Niesten MCEJ, Feijen J, Gaymans RJ. Polymer 2000;41:8487.
[8] van der Schuur M, de Boer J, Gaymans RJ. Polymer 2005;46:9243.
[9] Harrell LL. Macromolecules 1969;2:607.
[10] Ng HN, Allegrezza AE, Seymour RW, Cooper SL. Polymer 1973;14:225.
[11] Eisenbach CD, Baumgartner M, Gunter G. In: Lal J, Mark JE, editors. Advances in elastomer and rubber elasticity, vol. 51. New York: Plenum Press; 1985.
[12] Christenson CP, Harthock MA, Turner RB. J Polym Sci, Part B: Polym Phys 1986;24:1401.
[13] Eisenbach CD, Baumgartner M, Gunter C. Polym Prepr 1985;26:7.
[14] van der Schuur M, Feijen J, Gaymans R. J Polym 2005;46:4584.
[15] Yui N, Nojima K, Ogata N. Polym J 1985;17:969.
[16] Krijgsman J, Husken D, Gaymans RJ. Polymer 2003;44:7573.
[17] van der Schuur M, Gaymans RJ. Submitted for publication.
[18] Niesten MCEJ, Gaymans RJ. J Appl Polym Sci 2001;81:1372.
[19] Lothmar J, Meyer K, Goldbach G. Makromol Chem 1988;189:2053.
[20] Mallakpour SE, Sheikholeslami B. Polym Int 1999;48:41.
[21] Ubale VP, Sagar AD, Birajdar MV. J Appl Polym Sci 2001;79:566.
[22] Dechant J. Ultrarotspektroskopische untersuchungen an polymeren. Berlin: Akademie; 1972.
[23] Sung CSP, Schneider NS. Macromolecules 1975;81:68.
[24] Dounis DV, Wilkes GL. Polymer 1997;38:2819.
[25] Kaushiva BD, Wilkes GL. Polymer 2000;41:285.
[26] Johnson PC, Isocyanate reactions: nature, control and significance in manufacture of polyurethanes. In: Buist JM, Gudgeon H, editors. Advances in polyurethane technology; Elsevier, London 1970, p. 1–24.
[27] Sawyer LC, Grubb DT. Polymer microscopy. 2nd ed. London: Chapman & Hall; 1996.
[28] Sperling LH. Introduction to physical polymer science. 3rd ed. New York: Wiley; 2001.
[29] Halpin JC, Kardos JL. J Appl Phys 1972;5:2235.
[30] van der Schuur M, van der Heide E, Feijen J, Gaymans RJ. Polymer 2004; 45:2721.